

doi: 10.3788/gzxb20164505.0512001

# 平行转镜式光谱仪原理与误差容限分析

才啟胜<sup>1,2</sup>, 相里斌<sup>1,2</sup>, 方煜<sup>2</sup>, 谭政<sup>2</sup>

(1 中国科学技术大学 精密机械与精密仪器系, 合肥 230027)

(2 中国科学院光电研究院 计算光学成像技术重点实验室, 北京 100094)

**摘 要:**采用光路展开法, 利用调制度与相位误差两种判据, 分析平行转镜在转动过程中的晃动、平行转镜的平行度、定镜的倾斜误差以及视场角等因素对平行转镜式光谱仪误差容限的影响. 分析表明: 平行转镜的晃动是平行转镜式光谱仪最重要的影响因素, 但由于平行转镜的连续快速转动, 惯性的作用会显著降低转动过程中的晃动影响; 系统对平行转镜的平行度不敏感, 对定镜的倾斜与视场角的误差容限与传统迈克尔逊式光谱仪相同. 相对于传统直线往复运动式的光谱仪, 平行转镜式光谱仪具有更高的探测速度与稳定性. 同时, 误差容限分析也为该光谱仪的系统设计与装调提供了理论指导.

**关键词:**傅里叶变换光谱仪; 误差分析; 干涉图; 平行转镜

中图分类号: O433.1; O435.1

文献标识码: A

文章编号: 1004-4213(2016)05-0512001-6

## Principle and Tolerance Analysis of a Rotating Parallel-mirror-pair Spectrometer

CAI Qi-sheng<sup>1,2</sup>, XIANG-LI Bin<sup>1,2</sup>, FANG Yu<sup>2</sup>, TAN Zheng<sup>2</sup>

(1 Department of Precision Machinery and Precision Instrumentation, University of Science and Technology of China, Hefei 230027, China)

(2 Academy of Opto-Electronics, Chinese Academy of Sciences, Beijing 100094, China)

**Abstract:** The tolerance of a rotating parallel-mirror-pair spectrometer (RPMPS) and some other considerations are analyzed using the modulation depth and the phase error criterion. These include the vibration of the parallel-mirror-pair (PMP), the alignment error of the fixed end mirrors, the parallelism of the two rotating mirrors, and the field of view. The theoretical results show that the vibration of the PMP is the most sensitive factor to RPMPS. However, as an ultra rapid continuous rotational system, the rotation inertia will reduce the effect of the vibration dramatically. The RPMPS is less sensitive to the parallelism of the two rotating mirrors. The tolerance for the alignment error of the fixed end mirrors and the field of view are similar to the traditional Michelson interferometer. Compared to the traditional linear motion form spectrometer, the RPMPS is an ultra rapid scanning Fourier-transform spectrometer with stability advantages. These analyses will also give a theoretic guidance for system design and manufacture of RPMPS.

**Key words:** Fourier-transform spectrometer; Tolerance analysis; Interferogram; Parallel-mirror-pair

**OCIS Codes:** 120.3180; 120.6200; 300.6190

## 0 Introduction

For the temporally-modulated Fourier-Transform

Spectroscopy (FTS), the stability of the moving element is a key factor which can affect the accuracy of the retrieved spectrum. According to the motion form

**Foundation item:** China National Funds for Distinguished Young Scientists of NSFC (No. 61225024)

**First author:** CAI Qi-sheng(1988-), male, Ph. D. candidate, mainly focuses on Fourier transform imaging spectroscopy. Email: cqsc@mail.ustc.edu.cn

**Supervisor:** XIANG-LI Bin (1967-), male, professor, Ph. D. degree, mainly focuses on interference imaging spectroscopy. Email: xinagli@aoe.ac.cn

**Received:** Oct. 9, 2015; **Accepted:** Dec. 14, 2015

<http://www.photon.ac.cn>

of the moving element, temporally-modulated FTS can be sorted in two classes, one is based on linear motion and the other is based on rotational motion. The Michelson interferometer with a moving mirror is the first FTS based on linear motion<sup>[1]</sup>. It is very compact and small in principle, but the inclination of the flat moving mirror during the scanning may decrease the modulation depth of the interferogram<sup>[2]</sup>. The tilt angle of the moving mirror should be less than approximately  $\lambda/(8D)$ <sup>[3]</sup>, where  $\lambda$  is the wavelength and  $D$  is the diameter of the moving mirror. One solution for this drawback is adopting a dynamic alignment system<sup>[4]</sup>. But this increases the complexity of the system<sup>[5]</sup>. Another solution is replacing the moving mirror and the fixed mirror in the Michelson interferometer with cat's eye retroreflectors<sup>[6]</sup> or cube-corner retroreflectors<sup>[7-10]</sup>. As the linear motion form FTS has some drawbacks which are not easy to overcome, some scholars provide the rotational motion form FTS<sup>[11]</sup>, such as the swinging interferometer<sup>[12-13]</sup>, the carousel interferometer<sup>[5]</sup>, the high speed rotary spectrometer<sup>[14]</sup>, and the ultra-rapid-scanning interferometer<sup>[15-17]</sup>.

As it is well known, tolerance analysis is very important for FTS. Many scholars have studied the error limits in the rotary FTS<sup>[18-20]</sup>. In this paper, the tolerance analysis and some other considerations of a novel continuous rotary spectrometer, the Rotating Parallel-Mirror-Pairspectrometer (RPMPS)<sup>[21]</sup>, are presented. The RPMPS is also an ultra rapid scanning spectrometer. The Optical Path Difference (OPD) of RPMPS is produced by the rotational movement of the rotating Parallel-Mirror-Pair (PMP). The PMP is the only moving part in RPMPS, and it is the key element of this spectrometer. The tolerance analysis of the RPMPS include the vibration of the PMP, the alignment error of the fixed end mirrors, the parallelism of the two rotating mirrors, and the field of view. These tolerance analyses of the RPMPS will give a theoretic guidance for system design and manufacture of RPMPS.

## 1 Principle of RPMPS

A sketch of the optical layout of RPMPS is presented in Fig. 1. It consists of a collimating lens (L1), a collecting lens (L2), a beam splitter (BS), a wedged PMP, two fixed end mirrors (M3 and M4), and a detector. The two parallel mirrors (M1 and M2) that constitute the PMP are driven by the motor (M) and can rotate around the shaft on which they are fixed. The shaft is perpendicular to the beam splitter. The two fixed end mirrors are symmetric about the beam splitter and are perpendicular to the rays incident

to them respectively. There is a wedged angle  $\theta$  between the shaft and the normal direction of the PMP.

The rays collimated by the collimating lens (L1) are divided into two beams at the beam splitter. The transmission beam (beam I, as the dash line shows), reflected firstly by the rotating wedged mirror M1 and then by the rotating wedged mirror M2, is reflected back at the fixed end mirror M3. The reflected beam (beam II, as the dot dash line shows), reflected firstly by the rotating wedged mirror M2 and then by the rotating wedged mirror M1, is reflected back at the fixed end mirror M4. Then these two beams recombine at the beam splitter and enter the collecting lens (L2). Finally, they are received by the detector and the interference intensity is transformed into a useful electrical signal.

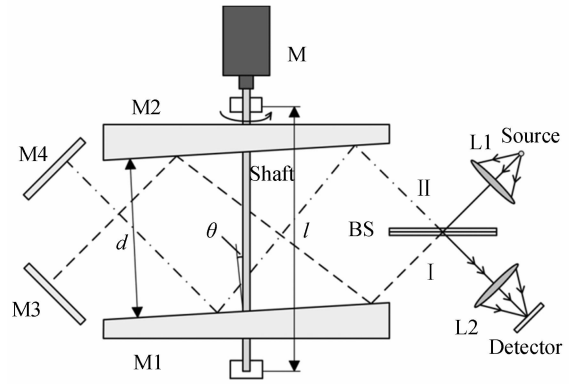


Fig. 1 Optical layout of the rotating PMP spectrometer

The OPD of the two beams is obtained by the rotational movement of the PMP. If the incident angle of the light on the beam splitter is  $45^\circ$ , the OPD is<sup>[21]</sup>

$$x = 4\sqrt{2}d \sin \theta \cos \beta \quad (1)$$

where  $d$  is the distance of the two parallel mirrors (as shown in Fig. 1),  $\theta$  is the wedged angle of the PMP, and  $\beta$  is the rotating angle of the PMP.

If the angular velocity of the PMP is  $\omega$ , we can rewrite the OPD as

$$x = F \cos(\omega t) \quad (2)$$

where

$$F = 4\sqrt{2}d \sin \theta \quad (3)$$

and  $t$  is the time. Fig. 2 shows the relationship between the OPD and the rotating angle of the PMP.

The interference intensity, as a function of the OPD, is the Fourier transform of the incident spectrum, and it can be written as

$$I(x) = \int_{\nu_1}^{\nu_2} B(\nu) \cos(2\pi \nu x) d\nu \quad (4)$$

where  $I(x)$  is the interference intensity,  $B(\nu)$  is the incident spectrum, and  $\nu$  denotes the wave number.

Substituting Eq. (2) into Eq. (4), we get

$$I(\beta) = \int_{\nu_1}^{\nu_2} B(\nu) \cos(2\pi \nu F \cos \beta) d\nu \quad (5)$$

Eq. (5) shows the relationship of the interference intensity and the rotating angle of the PMP. It is an even and periodic function, and the period is  $180^\circ$ .

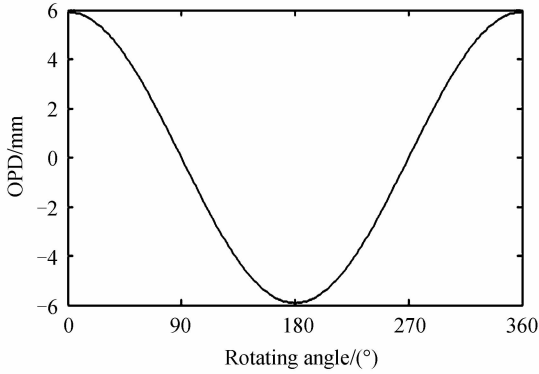


Fig. 2 Relationship between OPD and the rotating angle of the PMP ( $\theta=3^\circ$ ,  $d=20\text{mm}$ )

The reconstructed spectrum of the incident light is the inverse Fourier transform of the interferogram. The spectrum resolution depends on the maximum OPD.

$$B(\nu) = \int_{x_1}^{x_2} I(x) \cos(2\pi\nu x) dx \quad (6)$$

$$\delta\nu = \frac{1}{2L} \quad (7)$$

where  $\delta\nu$  is the spectrum resolution, and  $L$  is the maximum OPD.

## 2 Tolerance analyses

The OPD of this spectrometer is produced by rotary movement of the PMP. It is the only movable element and the most important part of this spectrometer. Vibration of the PMP is the main error during the rotation. The alignment of the two fixed end mirrors and the parallelism of the two parallel mirrors also bring errors to the interferogram. Some other effects are also considered in this section.

### 2.1 Vibration of the PMP

When the PMP rotates, tilt angle of the shaft will change due to the vibration. Suppose the tilt angle is  $\varphi$ , then the equivalent wedged angle of the PMP is  $\theta + \varphi$ . According to Eq. (1), we can get that the OPD is

$$x = 4\sqrt{2}d \sin(\theta + \varphi) \cos \beta \quad (8)$$

The error of the OPD produced by the vibration is

$$\Delta x = 4\sqrt{2}d \cos \beta [\sin(\theta + \varphi) - \sin \theta] \quad (9)$$

When the distance of the two parallel mirrors and the wedged angle of the PMP are fixed, Eq. (9) can be rewritten as  $\Delta x = \delta(\varphi, \beta)$ . If  $d=20\text{mm}$ , and  $\theta=3^\circ$ , this relationship is shown in Fig. 3.

When the vibration exists, the interference intensity of a monochromatic light is

$$I(x) = B(\nu) \cos[2\pi\nu(x + \Delta x)] \quad (10)$$

Eq. (10) shows that the vibration of the PMP brings phase error to the interferogram. This will

change the period of the interferogram. The change of the period should be less than  $\lambda/\text{SNR}$ <sup>[22]</sup>, that is

$$|\Delta \text{OPD}|_{\max} \leq \lambda/\text{SNR} \quad (11)$$

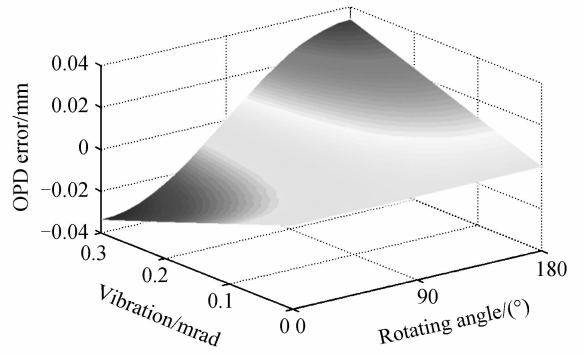


Fig. 3 Relationship between OPD error and vibration and rotating angle of PMP ( $\theta=3^\circ$ ,  $d=20\text{mm}$ )

If  $\lambda=25\ \mu\text{m}$ , and  $\text{SNR}=100$ . From Eq. (9) and Eq. (11), we can get

$$\varphi \leq 0.46'' \quad (12)$$

If the distance between the two bearings of the shaft is  $l$  (as shown in Fig. 1), the lateral play in the bearings should be less than  $l\varphi$ . If  $l=100\text{mm}$ , the maximal lateral play is  $0.22\ \mu\text{m}$ . This means that the spectrometer is sensitive to the vibration of the PMP. However, as a continuous rotational system, the rotate speed of the PMP is very fast. The rotation inertia will reduce the effect of the vibration dramatically. This is a major advantage of the rotational FTS compared to the linear FTS. Meanwhile, to reduce this sensitivity, we could set a larger distance between the two bearings ( $l$ ), shorten the separation of the two rotating mirrors ( $d$ ), or make this spectrometer work at a long-wavelength region.

### 2.2 Alignment error of the fixed end mirrors

Equivalent light path of this spectrometer is shown in Fig. 4. It is an unfolded form of Fig. 1. We can find that this spectrometer is evolved from a traditional Michelson interferometer. The OPD of a traditional Michelson interferometer is obtained by the

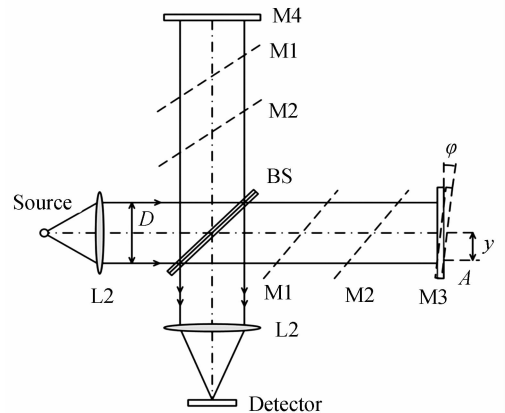


Fig. 4 Equivalent light path of the rotating PMP spectrometer with a tilted end mirror (M3)

translational movement of a reflecting mirror while in our spectrometer it is obtained by the rotational movement of the PMP. Because of this similarity, analysis for the alignment error of the end mirrors in our spectrometer can refer to the tilt analysis of the reflecting mirror in the Michelson interferometer.

In Fig. 4, L1 is the collimating lens and L2 is the collecting lens. M1 and M2 are the equivalents of the rotating mirrors in the two light paths. M3 and M4 are the two end mirrors.  $D$  is the beam diameter,  $A$  is the reclining center of end mirror (M3),  $y$  is the distance between  $A$  and the center of the incident beam, and  $\varphi$  is the tilt angle of M3. The additional OPD of the upper and lower side of the beam is

$$\Delta x \approx 2\varphi D \quad (13)$$

Suppose the aperture is rectangular, the interferogram is<sup>[23]</sup>

$$I(x) = \frac{1}{D} \int_{-(D/2-y)}^{D/2+y} B(\nu) \cos [2\pi\nu(x+2\varphi\zeta)] d\zeta = B(\nu) \text{sinc}(2\pi\nu D\varphi) \cos [2\pi\nu(x+2y\varphi)] \quad (14)$$

The modulation depth of the interferogram is  $\text{sinc}(2\pi\nu D\varphi)$ , and the initial phase is  $4\pi\nu y\varphi$ .

Tilt of the end mirror decreases the modulation depth and changes the period of the interferogram. The tilt tolerance is analyzed by means of modulation depth and phase error. The modulation depth of the interferogram should be greater than 90%<sup>[5]</sup>, and the change of the interferogram period resulting from the initial phase should be less than  $\lambda/\text{SNR}$ . We can get these two equations

$$\text{sinc}(2\pi\nu D\varphi) > 90\% \quad (15)$$

$$2y\varphi < \lambda/\text{SNR} \quad (16)$$

If  $\lambda = 25 \mu\text{m}$ , the diameter of the aperture is 10mm, and  $\text{SNR} = 100$ . We can get

$$\varphi < 1.07' \quad (17)$$

$$y < 0.4\text{mm} \quad (18)$$

These results show that, similar to the traditional Michelson interferometer, the alignment error of the end mirrors in RPMPS brings phase error to the interferogram and decrease the modulation depth. But different from the Michelson interferometer, the end mirrors in RPMPS are fixed. Thus, we only need to ensure their positional accuracy in the system alignment. This shows the stability advantage of the RPMPS.

### 2.3 Parallelism of the two rotating mirrors

When the two rotating mirrors are not parallel ideally, the direction of the rays incident to the end mirrors will not be perpendicular to them. Fig. 5 shows the equivalent light path of the RPMPS with a non-parallel rotating mirror (M2). If the tilt angle of M2 is  $\gamma$ , it is equivalent to that the two end mirrors M3 and M4 both have a tilt angle of  $2\gamma$  with opposite

directions. The emergent rays of the two light path have the same direction with an off-axis angle of  $4\gamma$ .

If the OPD is  $x$  under the ideal conditions, it will change to  $x[1 + \cos(4\gamma)]/2$  with M2 having a tilt angle of  $\gamma$ . According to Eq. (1), we can get that the error of the OPD produced by the non-parallel PMP is

$$\Delta x = x[\cos(4\gamma) - 1]/2 = 4\sqrt{2}d\sin\theta \cdot \cos\beta[\cos(4\gamma) - 1]/2 \quad (19)$$

As it is shown in Eq. (10), the non-parallel PMP brings phase error to the interferogram, which will change the period of the interferogram. The change of the period should be less than  $\lambda/\text{SNR}$ . If  $d = 20 \text{mm}$ ,  $\theta = 3^\circ$ ,  $\lambda = 25 \mu\text{m}$ , and  $\text{SNR} = 100$ . We can get

$$\gamma \leq 11.17' \quad (20)$$

The result shows that although the PMP is the key element in RPMPS, this spectrometer is less sensitive to the parallelism of the two rotating mirrors.

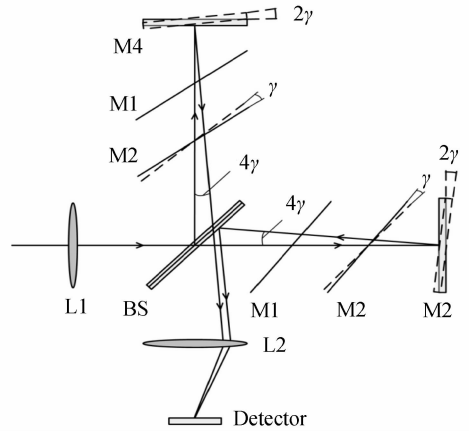


Fig. 5 Equivalent light path of the rotating PMP spectrometer with a non-parallel rotating mirror (M2)

### 2.4 Field of view

In the analyses above, we assume that the incident beam is an ideal collimated beam, which means the entrance aperture is a point located at the focus of the collimating lens. However, in order to get a measurable amount of radiation through the spectrometer, a finite aperture is needed. Then the collimated light traverses the spectrometer at a range of angles off-axis and the OPDs for different angles extends over a range of values rather than a single value for on-axis light. This will reduce the modulation depth of the interferogram. The equivalent light path of this spectrometer in Fig. 4 shows that the RPMPS is an evolved form of a traditional Michelson interferometer. If the OPD for on-axis light is  $x$ , then the OPD for off-axis light with angle  $\Delta\alpha$  is  $x\cos(\Delta\alpha)$ . To choose the diameter of the optimum aperture, we can refer to the analysis of the traditional Michelson interferometer. Suppose the solid angle of the radiation source is  $\Omega$ , and the resolving power is  $R$ , then the relationship between them is<sup>[1]</sup>

$$\Omega = \frac{2\pi}{R} \quad (21)$$

If the resolving power of this spectrometer is set as  $R=30\,000$ , we can get the solid angle is;

$$\Omega = 0.00021 \quad (22)$$

and the accepted off-axis angle is

$$\alpha = \sqrt{\Omega/\pi} = 0.008\text{rad} = 0.47^\circ \quad (23)$$

## 2.5 Other considerations

When this spectrometer is operated at a high resolving power, a calibration of the wavelength should be performed. A reference monochromatic light source could be set into this spectrometer. If the reference source and the under test source have the same incident direction, they will have the same OPD when the PMP is rotating. Then we can get two interferograms after the measurement is completed, one is the interferogram of the under test light and the other is a reference interferogram of a monochromatic light source. From the reference interferogram, the phase error and the modulation depth that are caused by the factors mentioned above can be calculated.

Another consideration is that the RPMPS has a fixed OPD range with a given instrument because of the fixed angle and separation of the two rotating mirrors. This means that it has an inflexible spectral resolution. This may be a less serious drawback of this spectrometer compared with a linear FTS where a shorter scan could be performed if lower spectral resolution is appropriate.

## 3 Conclusions

In this paper, the principle of the RPMPS is studied and the tolerance analyses of this spectrometer are given in detail. The tolerance analyses show that the vibration of the PMP during its rotation is the most sensitive factor to this spectrometer. However, as a continuous rotational system, the rotate speed of the PMP could be very fast and rotation inertia will reduce the effect of the vibration dramatically. This is a major advantage of the rotational FTS compared to the linear FTS. Similar to the traditional Michelson interferometer, the alignment error of the end mirrors in RPMPS brings phase error to the interferogram and decrease the modulation depth. But different from the traditional Michelson interferometer, the end mirrors in RPMPS is fixed. Thus, we only need to ensure their positional accuracy in the system alignment. This shows the stability advantage of the RPMPS. The RPMPS is less sensitive to the parallelism of the two rotating mirrors. For the field of view, it is same to the traditional Michelson interferometer.

The analyses show that the RPMPS is an ultra rapid scanning Fourier-transform spectrometer with

stability advantages. These analyses also give a theoretic guidance for system design and manufacture of RPMPS.

## References

- [1] DAVISS P, ABRAMSM C, BRAULTJ W. Fourier transform spectrometry[M]. Academic Press, 2001.
- [2] STROKEG W. Photoelectric fringe signal information and range in interferometers with moving mirrors[J]. *Journal of the Optical Society of America*, 1957, **47**(12):1097-1103.
- [3] YANG Qing-hua, ZHOU Ren-kui, ZHAO Bao-chang. Principle of the moving-mirror-pair interferometer and the tilt tolerance of the double moving mirror[J]. *Applied Optics*, 2008, **47**(13): 2486-2493.
- [4] KAUPPINEN J, HORNEMANV M. Dynamic alignment system of a Michelson interferometer [M]. University of Turku, 1989.
- [5] KAUPPINENJ K, SALOMAAI K, PARTANENJ O. Carousel interferometer[J]. *Applied Optics*, 1995, **34**(27), 6081-6085.
- [6] CONNES J, CONNES P. Near-infrared planetary spectra by Fourier spectroscopy. I: Instruments and results[J]. *Journal of the Optical Society of America*, 1966, **56**(7):896-910.
- [7] KAUPPINEN J, HORNEMAN V M. Large aperture cube corner interferometer with a resolution of 0.001 cm<sup>-1</sup>[J]. *Applied Optics*, 1991, **30**(18): 2575-2578.
- [8] KAUPPINEN J, SAARINEN P. Line-shape distortions in misaligned cube corner interferometers[J]. *Applied Optics*, 1992, **31**(1): 69-74.
- [9] KYRÖ E, KAUPPINEN J, JUNTILA M L, *et al.* Fourier transform wavemeter[J]. *Review of Scientific Instruments*, 1987, **58**:1180-1184.
- [10] YANG Qing-hua, ZHOU Ren-kui, ZHAO Bao-chang. Novel moving-corner-cube-pair interferometer[J]. *Journal of Optics A Pure & Applied Optics*, 2009, **11**(1): 15505-15509.
- [11] KAUPPINEN J, HEINONEN J, KAUPPINEN I. Interferometers based on the rotational motion[J]. *Applied Spectroscopy Reviews*, 2004, **39**(1): 99-130.
- [12] BRIERLEY P R. Interferometer spectrometer having tiltable reflector assembly and reflector assembly therefor. U. S. patent 4,915,502 (10 Apr. 1990).
- [13] YAZDI S, RASHIDIAN B. Two new swinging interferometers[J]. *Journal of Optics A: Pure and Applied Optics*, 2007, **9**(7):560 - 564.
- [14] WADSWORTH W, DYBWAD J P. Ultra high speed chemical imaging spectrometer[C]. SPIE, 1997, **3082**: 148-194.
- [15] GRIFFITHS P, HIRSCH B, MANNING C. Ultra-rapid-scanning Fourier transform infrared spectrometry [J]. *Vibrational Spectroscopy*, 1999, **19**(1):165-176.
- [16] WEI Ru-yi, ZHANG Xue-min, ZHOU Jin-song, *et al.* Calculations on optical path difference of a high resolution reflecting scanning Fourier transform spectrometry[J]. *Acta Optica Sinica*, 2011, **31**(7): 0730001.
- [17] ZHANG Wen-xi, XIANG-LI Bin, YUAN Yan, *et al.* Ultra-rapid-scanning imaging interferometer [J]. *Acta Photonica Sinica*, 2006, **35**(8): 1153-1155.
- [18] YANG Xiao-xu, ZHOU Si-zhong, XIANG-LI Bin. Studies of error limited of high speed rotary spectrometer [J]. *Acta Photonica Sinica*, 2004, **33**(3): 338-341.
- [19] GAO Xiao-feng, CUI Yan, XIANG-LI Bin. The tolerance of the end mirror tilting in high speed rotary spectrometer[J]. *Acta Photonica Sinica*, 2006, **35**(4): 614-617.

- [20] YUAN Yan, XIANG-LI Bin. Design consideration of rotary interference spectral imager (ROSI) [J]. *Acta Photonica Sinica*, 2007, **36**(2): 279-281.
- [21] CAI Qi-sheng, XIANG-LI Bin, FU Qiang, *et al.* Conceptual design of a rotating parallel-mirror-pair interferometer[C]. SPIE, 2014, **9142**: 9142I.
- [22] VAUGHANA H. Imaging Michelson spectrometer for Hubble Space Telescope[C]. SPIE, 1988, **1036**: 2-14.
- [23] XIANG-LI Bin, YANG Jian-feng, GAO Zhan, *et al.* On the tolerance of the mirror tilting in Fourier transform interferometer[J]. *Acta Photonica Sinica*, 1997, **26** (2): 132-135.